ISSN 1547-4771, Physics of Particles and Nuclei Letters, 2020, Vol. 17, No. 1, pp. 79–84. © Pleiades Publishing, Ltd., 2020.

PHYSICS OF SOLID STATE AND CONDENSED MATTER

Ferromagnetic Resonance and Effect of Supercurrent on the Magnetization Dynamics in S/F/S Junctions under Circularly Polarized Magnetic Field

M. Nashaat[a, b, *] and Yu. M. Shukrinov[a, c, **]

[a] *BLTP, JINR, Dubna, Moscow Region, 141980 Russia*

[b] *Department of Physics, Cairo University, Cairo, 12613 Egypt*

[c] *Dubna State University, Dubna, 141982 Russia*

**e-mail: majed@sci.cu.edu.eg*

***e-mail: shukrinv@theor.jinr.ru*

Received September 20, 2019; revised September 26, 2019; accepted September 26, 2019

Abstract—The coupling between the Josephson phase and magnetization in Superconductor/Ferromagnet/Superconductor (S/F/S) junctions plays an important role in the dynamics of this system. In the presence of this coupling, we demonstrate the manifestation of the ferromagnetic resonance (FMR) in the frequency dependence of the magnetization and critical current of S/F/S Josephson junction under circularly polarized magnetic field. Furthermore, we compare the simulation results in both the nonlinearized and the linearized models. The ferromagnetic resonance linewidth and the resonance frequency are strongly affected by the ratio of the Josephson and magnetic energies.

DOI: 10.1134/S1547477120010136

1. INTRODUCTION

Superconductor/Ferromagnet/superconductor (S/F/S) Josephson junction is widely considered to be the place where spintronics and superconductivity fields interact [1]. In these junctions the supercurrent induces magnetization dynamics due to the coupling between the Josephson and magnetic subsystems. The possibility of achieving electric control over the magnetic properties of the magnet via Josephson current and its counterpart, recently attracted a lot of attention [2–6]. In [4] the authors demonstrate a unique magnetization dynamics with a series of specific phase trajectories. The origin of these trajectories is related to a direct coupling between the magnetic moment and the Josephson oscillations in these junctions and ferromagnetic resonance (FMR) when Josephson frequency coincides with the ferromagnetic one.

In this paper, we study the coupling between the Josephson phase and the magnetization which can be achieved by electromagnetic field [7–14]. We present a detailed analysis of the effect of the Josephson energy on the FMR in S/F/S junction under circularly polarized magnetic field in case of nonlinearized and linearized Landau–Lifshitz–Gilbert (LLG) equation. The coupling between Josephson phase and magnetization alters the FMR linewidth and leads to a shift of the FMR frequency. We develop the model which takes into account the interaction between magnetization and Josephson phase in S/F/S junction under circularly polarized magnetic field using the Resistively Shunted Junction (RSJ) model. The simulation results are demonstrated for both the nonlinearized and the linearized cases.

2. MODEL AND METHODS

We consider two superconductors separated by ferromagnetic layer with thickness d as shown in Fig. 1. The area of the junction is $L_y L_z$ and a bias current flows in the x-direction. An uniaxial constant magnetic field H_0 is applied in z-direction, while a circularly polarized magnetic field is applied in xy-plane $\mathbf{H}_{ac} = (H_{ac}\cos\omega t, H_{ac}\sin\omega t, 0)$ with amplitude H_{ac} and frequency ω.

The current through the junction according to RSJ model in the dimensionless form can be written as [9, 14]:

$$I/I_c^0 = \frac{\sin(\phi_{sy} m_z)\sin(\phi_{sz} m_y)}{(\phi_{sy} m_z)(\phi_{sz} m_y)}\sin\theta + \frac{d\theta}{dt}, \qquad (1)$$

where I_c^0 is the critical current, $\phi_{sy} = 4\pi^2 L_y d\, M_0/\Phi_0$, $\phi_{sz} = 4\pi^2 l_z d\, M_0/\Phi_0$, Φ_0 is the flux quantum, $m_{y,z} = \mathbf{M}_{y,z}/M_0$, $M_0 = |\mathbf{M}|$ is the saturation magneti-

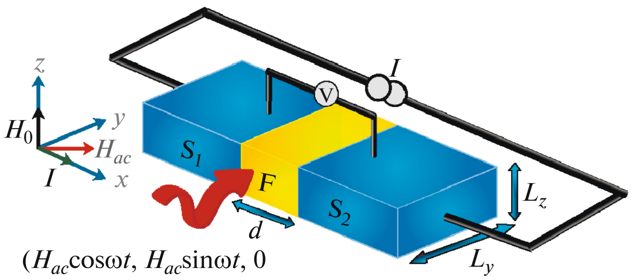

Fig. 1. Schematic diagram for S/F/S junction. The bias current is applied in x-direction, a circularly polarized microwave with amplitude H_{ac} and frequency ω is applied in xy-plane and an uniaxial constant magnetic field H_0 is applied in z-direction.

zation, t is normalized to ω_c^{-1}, and $\omega_c = 2\pi I_c^0 R/\Phi_0$ is the characteristic frequency. The dynamics of magnetization m_y and m_z in the considered junction are described by the LLG equation [14]:

$$\frac{d\mathbf{m}}{dt} = -\frac{\Omega_0}{(1+\alpha^2)}(\mathbf{m}\times\mathbf{h}_e + \alpha[\mathbf{m}\times(\mathbf{m}\times\mathbf{h}_e)]), \tag{2}$$

where $\Omega_0 = \omega_0/\omega_c$, ω_0 is the ferromagnetic resonance frequency, α is the Gilbert damping, $\mathbf{h}_e = \mathbf{H}_e/H_0$ is the normalized effective field, $H_0 = \omega_0/\gamma$, and γ is the gyromagnetic ratio. The total energy of the system is determined by

$$E = E_M + E_{ac} + E_s, \tag{3}$$

where E_M, E_{ac} are the energy of the constant *dc* and *ac* magnetic fields, respectively, and E_s is the Josephson energy. In the proposed system we have [14]:

$$\begin{gathered} E_s = -\frac{\Phi_0}{2\pi}\left(\theta(t) - \frac{8\pi^2 d}{\Phi_0}(M_z(t)y - M_y(t)z)\right)I \\ + E_J\left[1 - \cos\left(\theta(t) - \frac{8\pi^2 d}{\Phi_0}(M_z(t)y - M_y(t)z)\right)\right], \\ E_M = -vH_0M_z(t), \\ E_{ac} = -vM_x(t)H_{ac}\cos(\omega t) - vM_y(t)H_{ac}\sin(\omega t). \end{gathered} \tag{4}$$

Here v is the volume of the ferromagnetic layer, and $E_J = \Phi_0 I_c/2\pi$. The effective field is given by

$$\mathbf{H}_e = -\frac{1}{v}\nabla_{\mathbf{M}}E. \tag{5}$$

After integrating over the junction area, the total effective field in the dimensionless form reads as

$$\begin{gathered} \mathbf{h}_e = h_{ac}\cos(\Omega t)\hat{\mathbf{e}}_x + (h_{ac}\sin(\Omega t) + \Gamma_{ij}\epsilon_J\cos\theta) \\ \times\hat{\mathbf{e}}_y + (1 + \Gamma_{ji}\epsilon_J\cos\theta)\hat{\mathbf{e}}_z, \end{gathered} \tag{6}$$

with $\epsilon_J = E_J/(vM_0H_0)$ and

$$\Gamma_{ij} = \frac{\sin(\phi_{si}m_j)}{m_i(\phi_{si}m_j)}\left[\cos(\phi_{sj}m_i) - \frac{\sin(\phi_{sj}m_i)}{(\phi_{sj}m_i)}\right]\delta_J, \tag{7}$$

here the index $i = y, j = z$ and

$$\delta_J = \begin{cases} 0: \text{if } \mathbf{h}_e = 1 + \mathbf{h}_{ac}, \\ 1: \text{if } \mathbf{h}_e = 1 + \mathbf{h}_{ac} + \mathbf{h}_s. \end{cases}$$

In case of high-frequency magnetic susceptibility one can linearize LLG equation, then the RSJ equation is reduced to [14]:

$$I/I_c = \frac{\sin(\phi_s m_y)}{(\phi_s m_y)}\sin\theta(t) + \frac{d\theta(t)}{dt}, \tag{8}$$

where $I_c = I_c^0\sin(\phi_{sy})/(\phi_{sy})$, $\phi_{sy} = 4\pi^2 L_y d\,M_z/\Phi_0$ and the expression for y-component of magnetization has the form [14]:

$$m_{yl} = \frac{-2\alpha\frac{\Omega^2}{\Omega_0^2}\cos(\Omega t) + \left(1 - \eta_1\frac{\Omega^2}{\Omega_0^2}\right)\sin(\Omega t)}{\left(1 - \eta_2\frac{\Omega^2}{\Omega_0^2}\right)^2 + \Delta_J\left(1 - \eta_1\frac{\Omega^2}{\Omega_0^2}\right) + 4\alpha^2\frac{\Omega^2}{\Omega_0^2}}, \tag{9}$$

where $\Delta_J = \epsilon_J\phi_{sz}^2\cos\theta(t)/3$, $\eta_1 = 1 - \alpha^2$ and $\eta_2 = 1 + \alpha^2$ and $\phi_s = (4\pi^2 L_z d h_{ac} M_z)/(\Phi_0)$.

The magnetization and phase dynamics of the S/F/S junction can be described by solving Eq. (1) and Eq. (2) together. To solve this system of equations, we employ the fourth-order Runge–Kutta scheme. The initial conditions for the magnetization components are assumed to be $m_x = 0$, $m_y = 0.01$ and $m_z = \sqrt{1 - m_x^2 - m_y^2}$, while for the voltage and phase we have $V_{ini} = 0$, $\theta_{ini} = 0$.

3. RESULTS AND DISCUSSION

First, we investigate the effect of the Josephson energy on the FMR by comparing the FMR linewidth with $\delta_J = 0$, when $h_e = 1 + h_{ac}$ and $\delta_J = 1$, when $h_e = 1 + h_{ac} + h_s$. Figure 2 demonstrates the manifestation of FMR in the frequency dependence of the maximum amplitude of the magnetization component $m_y(t)$ and $m_z(t)$ ($m_x(t)$ is qualitatively same as $m_y(t)$). It illustrates the maximal amplitude of $m_y(t)$ versus Ω, while a minimum occurs for $m_z(t)$. At $\Delta_J = 0$ the linewidth is symmetric around the resonance frequency $\Omega_0 = 0.5$, however, at $\delta_J = 1$, the FMR linewidth is not symmetric. So, this fact reflects the influence of the Josephson energy to the effective field.

Next, we show the manifestation of FMR in the frequency dependence of the average critical current density. In the nonlinearized scheme the average critical current is given by

$$I_c = \left\langle\frac{\sin(\phi_{sy}m_z)\sin(\phi_{sz}m_y)}{(\phi_{sy}m_z)(\phi_{sz}m_y)}\right\rangle. \tag{10}$$

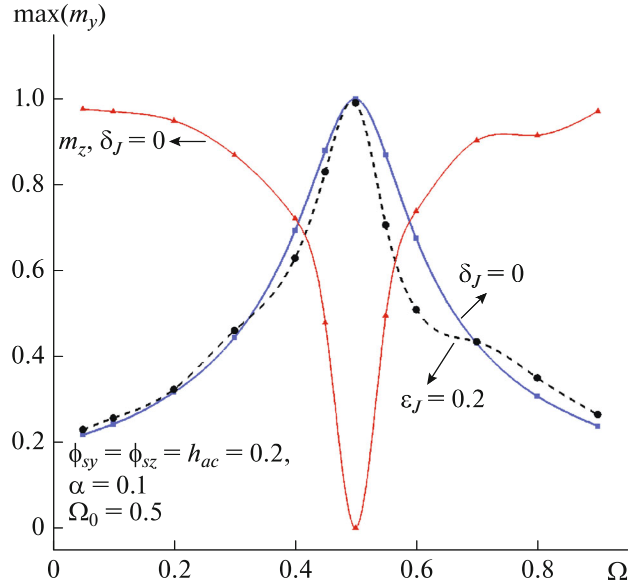

Fig. 2. Manifestation of the FMR in the frequency dependence of the maximum amplitude of the magnetization component m_y and m_z at bias current I = 1.16. Lines added to guide the eye.

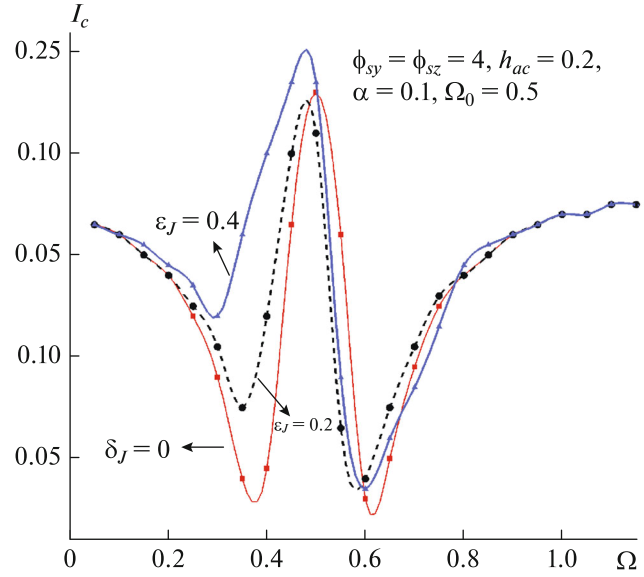

Fig. 3. Manifestation of the FMR in the frequency dependence of the average critical current density for three different values of ε_J.

The FMR linewidth at $\delta_J = 0$ and $\delta_J = 1$ is shown in Fig. 3. As we see, at $\delta_J = 1$ the resonance linewidth is getting not symmetric as the result of including Josephson energy to the effective field. Furthermore, the effect of increasing ε_J is manifested in a shift of the FMR frequency. The value of this shift is presented below, where the linearized LLG is considered.

In the linearized scheme, the resonance frequency can be found by analyzing the denominator of $m_y(t)$ (see Eq. (9)) which can be written in the following form

$$\Lambda = 1 + (1+\alpha^2)^2(\Omega/\Omega_0)^4 + 2(\alpha^2 - 1) \times (\Omega/\Omega_0)^2 + \Delta_J((\alpha^2 - 1)(\Omega/\Omega_0)^2 + 1). \tag{11}$$

At the resonance, the value of $m_y(t)$ is maximum, i.e., Λ has a minimum. So, we have to solve the equation $\frac{d\Lambda}{d\Omega} = 0$ for Ω_r to get the critical points. Then, to check if the resultant frequency corresponds to the minimum value for Λ, we find $\left.\frac{d^2\Lambda}{d\Omega^2}\right|_{\Omega_r}$. Four different cases are shown below for the resonance frequency Ω_r

$$\alpha = 0 \begin{cases} \Omega_r = \pm\Omega_0, & \Delta_J = 0, \\ \Omega_r = \pm\dfrac{\sqrt{2+\Delta_J}}{\sqrt{2}}\Omega_0, & \Delta_J \neq 0. \end{cases} \tag{12}$$

$$\alpha \neq 0 \begin{cases} \Omega_r = \pm\dfrac{\sqrt{1-\alpha^2}}{1+\alpha^2}\Omega_0, & \Delta_J = 0, \\ \Omega_r = \pm\dfrac{\sqrt{(1-\alpha^2)(2+\Delta_J)}}{\sqrt{2}(1+\alpha^2)}\Omega_0, & \Delta_J \neq 0. \end{cases} \tag{13}$$

The manifestation of FMR in the frequency dependence of the maximum amplitude of the magnetization component $m_y(t)$ is shown in Fig. 4 at different values of ε_J and α. In Figs. 4a and 4b we demonstrate the effect of ε_J on the resonance frequency at $\alpha = 0$. For clarity, we show an enlarged part for the maximum value of m_{yl} around $\Omega = 0.5$. At $\Delta_J = 0$, we observe singularity at $\Omega = \Omega_0$, which can be seen from the expression of m_y at $\alpha = 0$

$$m_{yl}(t) = \frac{3\Omega_0^2\sin(\Omega t)}{3(\Omega_0^2 - \Omega^2) + \Omega_0^2\epsilon_J\phi_{sz}^2\cos(\theta(t))}. \tag{14}$$

This singularity disappears at $\varepsilon_J \neq 0$, and $m_{yl}(t)$ has an upper limit for the maximal value which decreases with increasing ε_J (see Figs. 4b and Eq. (14)). Near the resonance, the conditions of linearization are violated, which is demonstrated by large values of m_{yl}, but nevertheless the used formulas could help to see the variation of resonance position, and the position of the Devil's staircase in the IV characteristics as demonstrated in [14]. Furthermore, the resonance linewidth becomes wider and the resonance frequency is shifted from $\Omega = \Omega_0$. In Fig. 4c we demonstrate the effect of α and ε_J on the resonance frequency and its linewidth. At $\alpha = 0.1$ the resonance linewidth is narrower than in case with $\alpha = 0.3$. However, at $\alpha = 0.1$ and $\varepsilon_J = 0.2$ the resonance linewidth is narrower than in case with $\varepsilon_J = 0.02$. In addition to this, the maximum value of $m_{yl}(t)$ for $\varepsilon_J = 0.2$ is larger than the case with $\varepsilon_J = 0.02$. This result is opposite to the case with $\alpha = 0$, where the maximum value increases with decreasing ε_J.

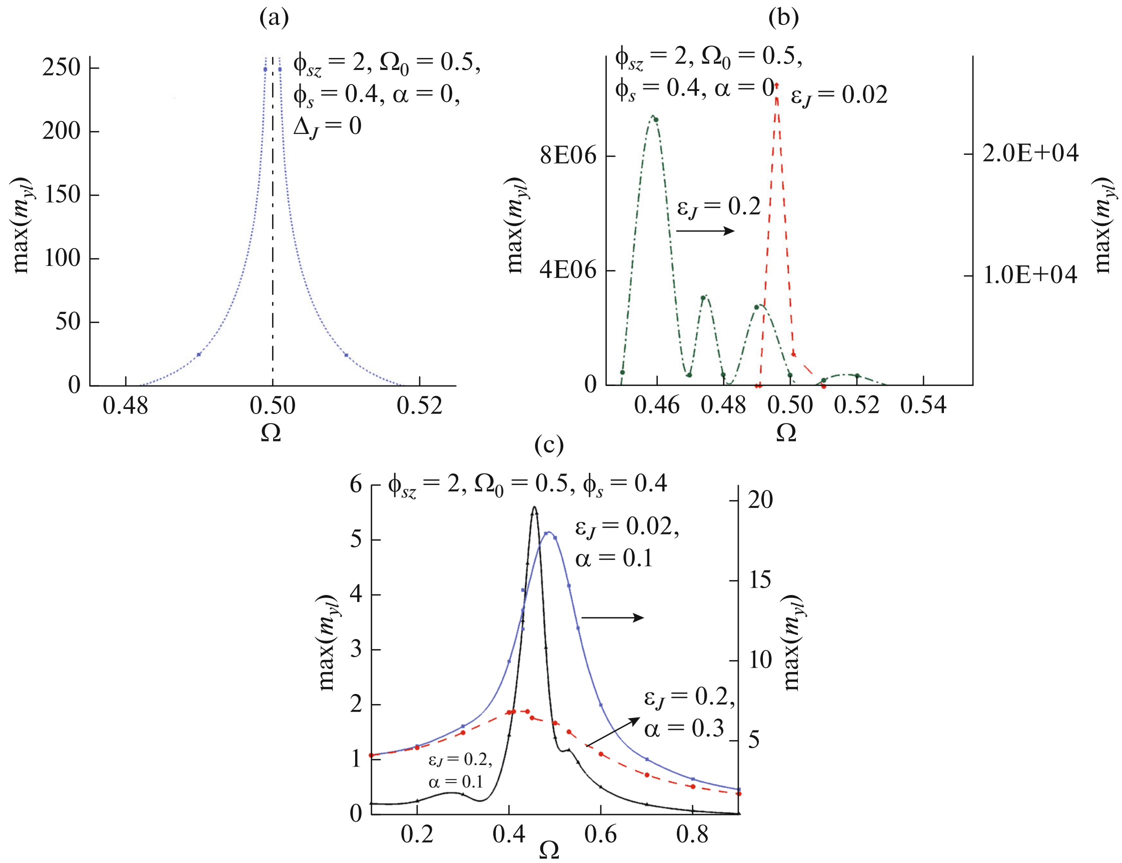

Fig. 4. Frequency dependence of the maximum amplitude of the magnetization component $m_y(t)$. (a) An enlarged part of the resonance curve is shown around $\Omega = 0.5$ at $\alpha = 0$. (b) The same as in (a), but with $\varepsilon_J \neq 0$. (c) The same as in (a), but with $\alpha \neq 0$.

A rough estimation for the resonance shift can be done using Eq. (12) for $\alpha = 0$ and Eq. (13) for $\alpha \neq 0$. Since $\Delta_J \propto \cos(\theta(t))$ and $|\cos\theta| \leq 1$, we can calculate the shift at the extreme limits in which $\cos\theta(t) = \pm 1$. We denote $\delta_L = |\Omega_0 - \Omega_L|$ as the left shift of the resonance frequency from Ω_0 with $\cos\theta = -1$, while $\delta_L = |\Omega_R - \Omega_0|$ is the right shift of the resonance frequency from Ω_0 with $\cos\theta = 1$. For the given parameters $\varphi_{sz} = 2$, $\varphi_s = 0.4$, and $\Omega_0 = 0.5$, the shift of the resonance frequency is presented in Table 1 at different values of ε_J and α.

All frequencies which are demonstrated in Table 1 correspond to the local minimum for Λ ($\left.\frac{d^2\Lambda}{d\Omega^2}\right|_{\Omega_r} > 0$). However, m_{yl} reaches a global maximum when $\cos\theta$

Table 1. Demonstration of the resonance frequency shift calculated from Eq. (14) at different values of ε_J with $\phi_{sz} = 2$, $\phi_s = 0.4$ and $\Omega_0 = 0.5$

α	ε_J	$\Omega_{r(L)}$, $\delta_L = \lvert\Omega_0 - \Omega_{r(L)}\rvert$, $\cos\theta = -1$	$\Omega_{r(R)}$, $\delta_R = \lvert\Omega_{r(R)} - \Omega_0\rvert$, $\cos\theta = 1$
0	0.002	$\Omega_{r(L)} = 0.4997$, $\delta_L = 0.0003$	$\Omega_{r(R)} = 0.5003$, $\delta_R = 0.0003$
0	0.2	$\Omega_{r(L)} = 0.4655$, $\delta_L = 0.0345$	$\Omega_{r(R)} = 0.5323$, $\delta_R = 0.0323$
0.1	0.02	$\Omega_{r(L1)} = 0.4893$, $\delta_{L1} = 0.0107$ $\Omega_{r(L2)} = 0.4958$, $\delta_{L2} = 0.0042$	No resonance at $\Omega_r > \Omega_0$
0.1	0.2	$\Omega_{r(L)} = 0.4585$, $\delta_L = 0.0415$	$\Omega_{r(R)} = 0.5244$, $\delta_R = 0.0244$
0.3	0.2	$\Omega_{r(L1)} = 0.4074$, $\delta_{L1} = 0.0927$ $\Omega_{r(L2)} = 0.4658$, $\delta_{L2} = 0.0342$	No resonance at $\Omega_r > \Omega_0$

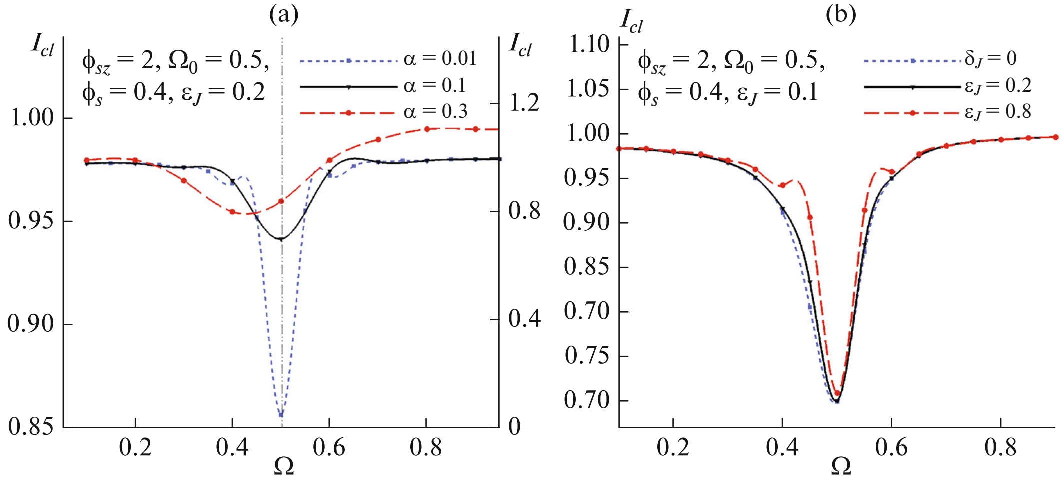

Fig. 5. Frequency dependence of the average critical current density I_{cl} in the linearized scheme. (a) Shows the effect of α on the FMR linewidth. (b) The same as in (a), but with different values of ε_J.

becomes negative such that the denominator has minimum (see Eq. (14)). The position of this global maximum occurs at the left of Ω_0, when $\cos\theta(t) = -1$. As shown in Fig. 4b, for $\varepsilon_J = 0.2$ we have two maximums with the global one at the left ($\Omega \approx 0.46$). One should note that we may have several local maximums in m_y depending on the value of $\cos\theta(t)$. Next, if $\alpha \neq 0$, both resonance frequencies with $\cos\theta = \pm 1$ may occur on the left side of Ω_0 as in the case with $\alpha = 0.1$ and 0.3. As we see, the position of the resonance frequency does not depend on the sign of $\cos\theta$ as in compare with $\alpha = 0$ case.

Next, in Fig. 5 we demonstrate the manifestation of the FMR in the frequency dependence of the average critical current I_{cl} in the linearized scheme. In this case it takes the form

$$I_{cl} = \left\langle \frac{\sin(\phi_s m_{yl})}{(\phi_s m_{yl})} \right\rangle. \tag{15}$$

Figure 5a shows how the resonance width is affected by changing α. At $\alpha = 0.01$, the resonance width is very narrow around Ω_0, while it becomes wider at $\alpha = 0.1$ and at $\alpha = 0.3$. A clear shift occurs for $\alpha = 0.3$. At the given numerical parameter, the minimum value for I_{cl} increases with increasing α. For $\alpha = 0.01, 0.1, 0.3$, the minimum occurs at $0.2, 0.7, 0.95$, respectively. The effect of ϵ_J is shown in Fig. 5b, where we observe a small variation for the FMR line width with changing ϵ_J. The mismatch in the behavior of I_c for linarized and nonlinearized cases is due to the different relations for the average critical current. In linearized case it is a function of $m_{yl}(t)$ only, so, the maximum of $m_{yl}(t)$ corresponds to the minimum of the critical current. On the other hand, for the nonlinearized case the critical current is function of additional terms with $m_z(t)$, which show a minimum at FMR. So, the total current in this case is determined by the competition between the maximum of m_y and minimum of $m_z(t)$.

Finally, we compare the resonance linewidth in case of the linearized and nonlinearized system of equations. We choose the same parameters for both systems. As shown in Fig. 6, the resonance linewidth for a linearized system is narrower than for nonlinear-

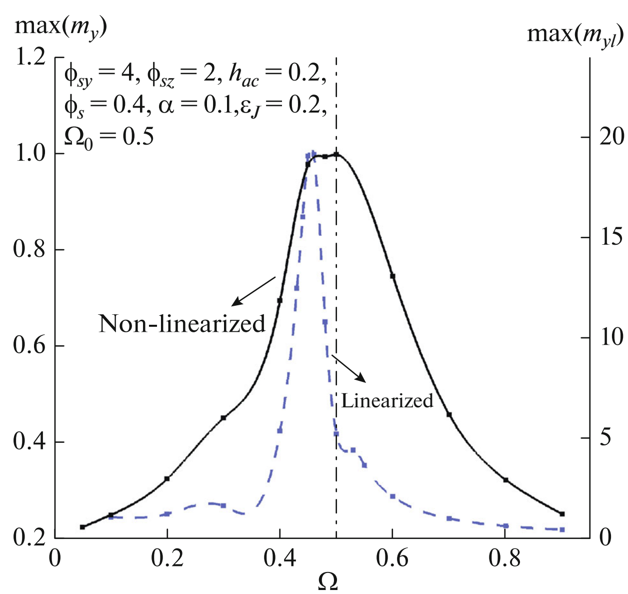

Fig. 6. Maximal amplitude of the m_y-component as a function of the magnetic field frequency in the nonlinearized ($\max(m_y)$) and linearized ($\max(m_{yl})$) cases.

ized one. Also, the shift from Ω_0 is very clear manifested for linearized system.

In conclusion, we have demonstrated the manifestation of ferromagnetic resonance in the frequency dependence of the magnetization amplitude and the average critical current density in S/F/S structure under circularly polarized magnetic field. The coupling between Josephson phase and magnetization affect the FMR linewidth and leads to the shift of the FMR frequency.

ACKNOWLEDGMENTS

The authors thank I. Rahmonov for fruitful discussions and Prof. D. Kamanin for supporting this work. The reported study was partially funded by the RFBR research projects 18-02-00318, 18-52-45011-IND, Egypt-JINR collaboration projects. Numerical calculations have been made in the framework of the RSF project 18-71-10095.

REFERENCES

1. J. Linder and K. Halterman, "Superconducting spintronics with magnetic domain walls," Phys. Rev. B **90**, 104502 (2014).
2. Yu. M. Shukrinov, I. R. Rahmonov, K. Sengupta, and A. Buzdin, "Magnetization reversal by superconducting current in ϕ_0 Josephson junctions," Appl. Phys. Lett. **110**, 182407 (2017).
3. S. Hikino, "Magnetization reversal by tuning Rashba spin-orbit interaction and Josephson phase in a ferromagnetic Josephson junction," J. Phys. Soc. Jpn. **87**, 074707 (2018).
4. Yu. M. Shukrinov, I. R. Rahmonov, and K. Sengupta, "Ferromagnetic resonance and magnetic precessions in ϕ_0 junctions," Phys. Rev. B **99**, 224513 (2019).
5. M. A. Silaev, I. V. Tokatly, and F. S. Bergeret, "Anomalous current in diffusive ferromagnetic Josephson junctions," Phys. Rev. B **95**, 184508 (2017).
6. I. V. Bobkova, A. M. Bobkov, and M. A. Silaev, "Gauge theory of the long-range proximity effect and spontaneous currents in superconducting heterostructures with strong ferromagnets," Phys. Rev. B **96**, 094506 (2017).
7. M. Weides, M. Kemmler, H. Kohlstedt, R. Waser, D. Koelle, R. Kleiner, and E. Goldobin, "0–π Josephson tunnel junctions with ferromagnetic barrier," Phys. Rev. Lett. **97**, 247001 (2006).
8. J. Pfeiffer, M. Kemmler, D. Koelle, R. Kleiner, E. Goldobin, M. Weides, A. K. Feofanov, J. Lisenfeld, and A. V. Ustinov, "Static and dynamic properties of 0,π and 0–π ferromagnetic Josephson tunnel junctions," Phys. Rev. B **77**, 214506 (2008).
9. S. Hikino, M. Mori, S. Takahashi, and S. Maekawa, "Microwave-induced supercurrent in a ferromagnetic Josephson junction," Supercond. Sci. Technol. **24**, 024008 (2011).
10. G. Wild, C. Probst, A. Marx, and R. Gross, "Josephson coupling and fiske dynamics in ferromagnetic tunnel junctions," Eur. Phys. J. B **78**, 509–523 (2010).
11. M. Kemmler, M. Weides, M. Weiler, M. Opel, S. T. B. Goennenwein, A. S. Vasenko, A. A. Golubov, H. Kohlstedt, D. Koelle, R. Kleiner, and E. Goldobin, "Magnetic interference patterns in 0–π superconductor/insulator/ferromagnet/superconductor Josephson junctions: effects of asymmetry between 0 and π regions," Phys. Rev. B **81**, 054522 (2010).
12. A. F. Volkov and K. B. Efetov, "Hybridization of spin and plasma waves in Josephson tunnel junctions containing a ferromagnetic layer," Phys. Rev. Lett. **103**, 037003 (2009).
13. S. Mai, E. Kandelaki, A. F. Volkov, and K. B. Efetov, "Interaction of Josephson and magnetic oscillations in Josephson tunnel junctions with a ferromagnetic layer," Phys. Rev. B **84**, 144519 (2011).
14. M. Nashaat, A. E. Botha, and Yu. M. Shukrinov, "Devil's staircases in the IV characteristics of superconductor/ferromagnet/superconductor Josephson junctions," Phys. Rev. B **97**, 224514 (2018).